

This is the accepted manuscript made available via CHORUS. The article has been published as:

Spin-Orbit Coupling Induced Spin-Transfer Torque and Current Polarization in Topological-Insulator/Ferromagnet Vertical Heterostructures

Farzad Mahfouzi, Naoto Nagaosa, and Branislav K. Nikolić

Phys. Rev. Lett. **109**, 166602 — Published 17 October 2012

DOI: [10.1103/PhysRevLett.109.166602](https://doi.org/10.1103/PhysRevLett.109.166602)

Spin-orbit coupling induced spin-transfer torque and current polarization in topological-insulator/ferromagnet vertical heterostructures

Farzad Mahfouzi,¹ Naoto Nagaosa,^{2,3} and Branislav K. Nikolić^{1,2,*}

¹*Department of Physics and Astronomy, University of Delaware, Newark, DE 19716-2570, USA*

²*Cross-Correlated Materials Research Group (CMRG) and Correlated Electron Research Group (CERG), RIKEN-ASI, Wako, Saitama 351-0198, Japan*

³*Department of Applied Physics, University of Tokyo, Tokyo 113-8656, Japan*

We predict an *unconventional* spin-transfer torque (STT) acting on the magnetization of a free ferromagnetic (F) layer within N/TI/F *vertical* heterostructures, which originates from strong spin-orbit coupling (SOC) on the surface of a three-dimensional topological insulator (TI), as well as from charge current becoming spin-polarized in the direction of transport as it flows perpendicularly from the normal metal (N) across the bulk of the TI layer. The STT vector has both the in-plane and the perpendicular components that are comparable in magnitude to conventional torque in F'/I/F magnetic tunnel junctions, while *not requiring* additional spin-polarizing F' layers with fixed magnetization, which makes it advantageous for spintronics applications. Our principal formal result is a derivation of the nonequilibrium Green function-based formula, and the corresponding gauge invariant nonequilibrium density matrix, which makes it possible to analyze the components of the STT vector in the presence of arbitrary SOC either in the bulk or at the interface of the free F layer.

PACS numbers: 72.25.Mk, 75.70.Tj, 85.75.-d, 72.10.Bg

The spin-transfer torque (STT) is a phenomenon in which spin current of large enough density injected into a ferromagnetic (F) layer either switches its magnetization from one static configuration to another or generates a dynamical situation with steady-state precessing magnetization [1]. The origin of STT is absorption of itinerant flow of angular momentum components normal to the magnetization direction. It represents one of the *central phenomena* of the second-generation spintronics, focused on manipulation of coherent spin states, since reduction of current densities (currently of the order 10^6 - 10^8 A/cm²) required for STT-based magnetization switching is expected to bring commercially viable magnetic random access memory (MRAM) [2]. The rich nonequilibrium physics [3] arising in the interplay of spin currents carried by fast conduction electrons and collective magnetization dynamics, viewed as the slow classical degree of freedom, is of great fundamental interest.

Very recent experiments [4, 5] and theoretical studies [6] have sought STT in nontraditional setups which do not involve the usual two (spin-polarizing and free) F layers with noncollinear magnetizations [3], but rely instead on the spin-orbit coupling (SOC) effects in structures lacking inversion symmetry. Such “SO torques” [7] have been detected [4] in Pt/Co/AlO_x lateral devices where current flows in the plane of Co layer. Concurrently, the recent discovery [8] of three-dimensional (3D) topological insulators (TIs), which possess a usual band gap in the bulk while hosting metallic surfaces whose massless Dirac electrons have spins locked with their momenta due to the strong Rashba-type SOC, has led to theoretical proposals to employ these exotic states of matter for spintronics [9] and STT in particular [10]. For example, magnetization of a ferromagnetic film with perpendicular

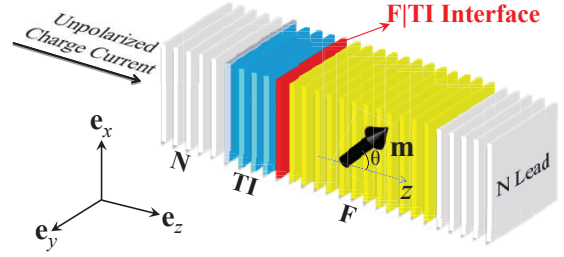


FIG. 1. (Color online) Schematic view of the topological-insulator-based vertical heterostructure operated by spin-transfer torque. The junction contains a *single* F layer of finite thickness with free magnetization \mathbf{m} , and the N leads are semi-infinite. We assume that each layer is composed of atomic monolayers (modeled on an infinite square tight-binding lattice).

anisotropy deposited on the TI surface could be switched by interfacial quantum Hall current [10]. However, very little is known about STT in setups where *spin transport is perpendicular* to interfaces with strong SOC [11–13], as exemplified by the vertical TI-based heterostructure in Fig. 1. Such heterostructures could exploit strong interfacial SOC without requiring [13, 14] perfectly insulating bulk whose unintentional doping in present experiments obscures [15] topological properties anticipated for lateral transport along the TI surface.

In this Letter, we predict that heterostructure in Fig. 1 will exhibit an *unconventional* STT, driven both by the surface SOC and spin-polarizing effect of the bulk of TI slab on current flowing perpendicularly through it. Its unusual features depicted in Fig. 2(a) could also open new avenues in the design of STT-MRAM [16] and spin torque oscillators [17]. For example, in conventional collinearly

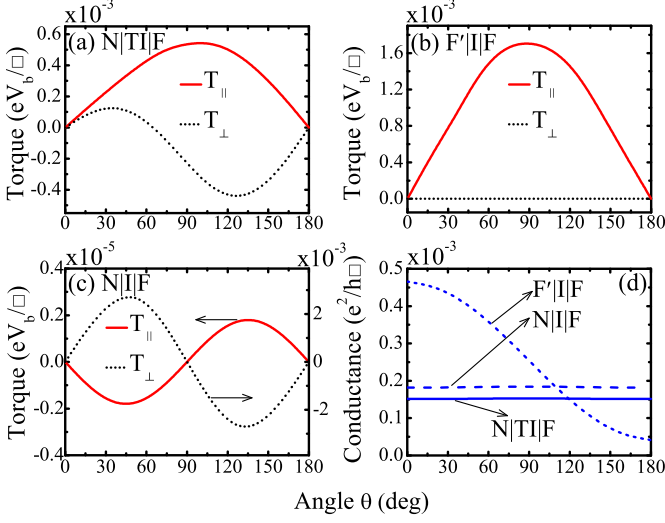


FIG. 2. (Color online) (a) The angular dependence of torque components, $\mathbf{T}_{\parallel} = \tau_{\parallel} \mathbf{m} \times (\mathbf{m} \times \mathbf{e}_z)$ and $\mathbf{T}_{\perp} = \tau_{\perp} \mathbf{m} \times \mathbf{e}_z$, acting on the free magnetization \mathbf{m} within N/TI/F heterostructure in Fig. 1. (b) The torque components, $\mathbf{T}_{\parallel} = \tau_{\parallel} \mathbf{m} \times (\mathbf{m} \times \mathbf{m}')$ and $\mathbf{T}_{\perp} = \tau_{\perp} \mathbf{m} \times \mathbf{m}'$, acting on the free-layer magnetization $\mathbf{m} = (\sin \theta \cos \phi, \sin \theta \sin \phi, \cos \theta)$ in conventional F'/I/F symmetric MTJ where magnetization of the reference layer F' is fixed at $\mathbf{m}' = \mathbf{e}_z$. (c) The torque components in N/I/F junction, defined in the same fashion as in panel (a), with the Rashba SOC of strength $\alpha_R/2a = 0.1$ eV located on the last monolayer of F which is in contact with I barrier. (d) The angular dependence of conductances for N/TI/F, F'/I/F and N/I/F junctions. The bias voltage V_b in all panels is sufficiently small to ensure the linear-response regime.

magnetized STT-MRAM devices [2], the initial current-induced STT is zero so that one has to rely on thermal fluctuations or small misalignments of the layer magnetizations to initiate the switching. Such undesirable long mean switching times and broad switching time distributions can be avoided by adding a TI capping layer onto the standard F/I/F' magnetic tunnel junction (MTJ), to form a TI/F/I/F' vertical heterostructure (see Sec. II in [18]), where TI layer will initiate fast switching of the F layer magnetization in accord with Fig. 2(a).

Our second principal result is a nonequilibrium Green function (NEGF)-based formula, and the related gauge invariant nonequilibrium density matrix (see Sec. III in [18]), which makes it possible to analyze the torque components in the presence of arbitrary spin-current non-conserving interactions within the device. Unlike the recently developed approaches [19, 20] to STT in the presence of SOC for the linear-response regime, ours can handle torque driven by finite bias voltage (required to reach sufficient current density in MTJs [3]), and it can also be easily combined with density functional theory (DFT) through the NEGF-DFT formalism [21, 22].

For conventional F'/I/F MTJs, where the reference F' layer with fixed magnetization \mathbf{m}' plays the role of an

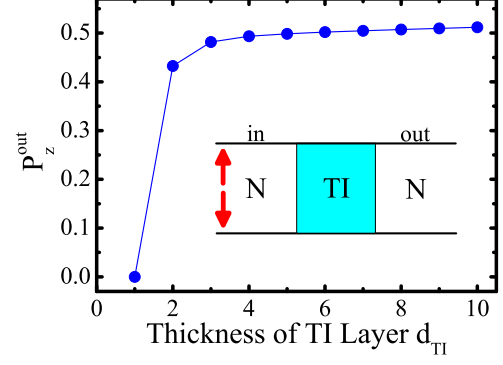


FIG. 3. (Color online) The spin-polarization vector $\mathbf{P}^{\text{out}} = (0, 0, P_z^{\text{out}})$ of current [28] in the right N lead of N/TI/N junction as a function of the thickness d_{TI} of the 3D TI layer after unpolarized charge current is injected from the left N lead.

external spin-polarizer, it is customary to analyze the in-plane (originally considered by Slonczewski [23]) and perpendicular (also called “field-like torque” [1]) components of the STT vector [3], $\mathbf{T} = \mathbf{T}_{\parallel} + \mathbf{T}_{\perp}$. The in-plane torque $\mathbf{T}_{\parallel} = \tau_{\parallel} \mathbf{m} \times (\mathbf{m} \times \mathbf{m}')$ is purely nonequilibrium and competes with the damping. The perpendicular torque $\mathbf{T}_{\perp} = \tau_{\perp} \mathbf{m} \times \mathbf{m}'$ arises from spin reorientation at the interfaces and possesses both equilibrium (i.e., interlayer exchange coupling) and nonequilibrium contributions which act like an effective magnetic field on the magnetization \mathbf{m} of the free F layer. While \mathbf{T}_{\perp} component is vanishingly small in metallic spin valves [24, 25], it can be substantial [3] in MTJs due to the momentum filtering imposed by the tunnel barrier [26, 27].

To understand the origin of torque components in Fig. 2(a), we first elucidate the effect of TI slab on unpolarized charge current injected from the left N lead by computing the spin density matrix $\hat{\rho}_{\text{spin}}^{\text{out}} = \frac{1}{2}(1 + \mathbf{P}^{\text{out}} \cdot \hat{\boldsymbol{\sigma}})$ for an ensemble of outgoing spin in the right normal metal (N) lead of N/TI/N junction. The expression for $\hat{\rho}_{\text{spin}}^{\text{out}}$, or equivalent spin-polarization vector \mathbf{P}^{out} , was derived as Eq. (10) in Ref. [28] in terms of the transmission matrix of the device. Its evaluation for N/TI/N junction is plotted in Fig. 3, which shows how TI slab polarizes the incoming current in the direction of transport with $\mathbf{P}^{\text{out}} = (0, 0, \simeq 0.5)$. The polarizing effect of the TI slab comes from the effective momentum-dependent magnetic field along the z -axis [encoded by the Γ_3 term in the TI Hamiltonian in Eq. (3) discussed below]. This requires sufficient thickness of the TI slab, as well as that the Fermi energy of the device E_F is within the bulk gap of TI. The spin-polarization of charge current induced by its flow through a finite-size region with SOC has been discussed previously for low-dimensional systems (such as the two-dimensional electron gas with the Rashba SOC [29]). Due to constraints imposed by the

time-reversal invariance, such SOC-induced polarization cannot [29] be detected via current or voltage measurement on standard two-terminal ferromagnetic circuits, as exemplified by Fig. 2(d) where conductance of N/TI/F junction is the same for $\mathbf{m} \parallel \mathbf{e}_z$ and $\mathbf{m} \nparallel \mathbf{e}_z$ configurations.

Following this analysis, the meaning of torque components in Fig. 2(a) for N/TI/F junction is explained by

$$\mathbf{T} = \mathbf{T}_{\parallel} + \mathbf{T}_{\perp} = \tau_{\parallel} \mathbf{m} \times (\mathbf{m} \times \mathbf{e}_z) + \tau_{\perp} \mathbf{m} \times \mathbf{e}_z. \quad (1)$$

The non-zero values of both \mathbf{T}_{\parallel} and \mathbf{T}_{\perp} in N/TI/F junction make this SOC-driven STT quite different from recently explored “SO torques” [6, 7] which lack anti-damping (i.e., equivalent to our \mathbf{T}_{\parallel}) component and, therefore, cannot induce precession of magnetization in the single F layer. We note that the same definition of torque components is applicable [12] also to N/I/F vertical heterostructures with strong Rashba SOC, $\alpha_R(\hat{\sigma} \times \mathbf{k}_{\parallel}) \cdot \mathbf{e}_z$, at the I/F interface [4, 7] even though current does not become polarized along \mathbf{e}_z there. The torque components for N/I/F junction plotted in Fig. 2(c) are driven purely by the surface Rashba SOC, which is the second order effect $\propto \alpha_R^2$ characterized by torque asymmetry [12] around the stable magnetic state $\theta = 90^\circ$. On the other hand, \mathbf{T}_{\parallel} and \mathbf{T}_{\perp} in Fig. 2(a) are non-zero at $\theta = 90^\circ$ in N/TI/F junctions due to the summation (see Sec. I in [18]) of an asymmetric contribution driven by the strong SOC on the surface of TI layer and a symmetric one [akin to conventional torque in MTJs shown in Fig. 2(b)] driven by spin-polarization [Fig. 3] of current flowing through the bulk of the TI layer.

Figures 2(a),(b) show that linear-response \mathbf{T}_{\parallel} in N/TI/F junctions is comparable to the one in symmetric F'/I/F MTJs tuned (via the on-site potential in the I layer) to have similar conductance, which points to unforeseen [9] spintronics applications of TIs. The angular dependence of conductances for N/TI/F, N/I/F, and F'/I/F junctions are compared in Fig. 2(d).

We now turn to details of our formalism. The junction in Fig. 1 is modeled on a cubic lattice, with lattice constant a and unit area $a^2 \equiv \square$, where monolayers of different materials (N, F, TI) are infinite in the transverse xy -direction. The TI layer has thickness $d_{\text{TI}} = 5$ and the free F layer has thickness $d_F = 70$ monolayers. The F and N layers are described by a tight-binding Hamiltonian with a single s -orbital per site

$$\begin{aligned} \hat{H}_F = & \sum_{n,\sigma\sigma',\mathbf{k}_{\parallel}} \hat{c}_{n\sigma,\mathbf{k}_{\parallel}}^\dagger \left(\varepsilon_{n,\mathbf{k}_{\parallel}} \delta_{\sigma\sigma'} - \frac{\Delta_n}{2} \mathbf{m} \cdot [\hat{\sigma}]_{\sigma\sigma'} \right) \hat{c}_{n\sigma',\mathbf{k}_{\parallel}} \\ & - \gamma \sum_{n,\sigma,\mathbf{k}_{\parallel}} (\hat{c}_{n\sigma,\mathbf{k}_{\parallel}}^\dagger \hat{c}_{n+1,\sigma,\mathbf{k}_{\parallel}} + \text{H.c.}). \end{aligned} \quad (2)$$

The operators $\hat{c}_{n\sigma}^\dagger$ ($\hat{c}_{n\sigma}$) create (annihilate) electron with spin σ on monolayer n with transverse momentum \mathbf{k}_{\parallel} within the monolayer. The in-monolayer kinetic energy

$\varepsilon_{n,\mathbf{k}_{\parallel}} = -2\gamma(\cos k_y a + \cos k_z a)$ is equivalent to an increase in the on-site energy, and the nearest neighbor hopping is $\gamma = 1.0$ eV. The coupling of itinerant electrons to collective magnetization dynamics is described through the material-dependent exchange potential $\Delta_n = 1.0$ eV ($\Delta_n \equiv 0$ within semi-infinite ideal N leads), where $\hat{\sigma} = (\hat{\sigma}_x, \hat{\sigma}_y, \hat{\sigma}_z)$ is the vector of the Pauli matrices and $[\hat{\sigma}_\alpha]_{\sigma\sigma'}$ denotes the Pauli matrix elements.

The minimal model for the slab of 3D TI, such as Bi_2Se_3 , is the effective tight-binding Hamiltonian with four orbitals per site [30]:

$$\begin{aligned} \hat{H}_{\text{TI}} = & \sum_{n,\mathbf{k}_{\parallel}} \left\{ \mathbf{c}_{n,\mathbf{k}_{\parallel}}^\dagger \left(\frac{B}{a^2} \Gamma_0 - i \frac{A}{2a} \Gamma_3 \right) \mathbf{c}_{n+1,\mathbf{k}_{\parallel}} + \text{H.c.} \right. \\ & \left. + \mathbf{c}_{n,\mathbf{k}_{\parallel}}^\dagger \left[C \mathbf{1} + d(\mathbf{k}_{\parallel}) \Gamma_0 + \frac{A}{a} (\Gamma_1 \sin k_x a + \Gamma_2 \sin k_y a) \right] \mathbf{c}_{n,\mathbf{k}_{\parallel}} \right\}. \end{aligned}$$

It yields the correct gap size in the bulk and surface dispersion while reducing to the continuum $\mathbf{k} \cdot \mathbf{p}$ Hamiltonian in the small k limit. Here $\hat{\mathbf{c}} = (\hat{c}_{+\uparrow}, \hat{c}_{+\downarrow}, \hat{c}_{-\uparrow}, \hat{c}_{-\downarrow})^T$ annihilates electron in different orbitals, $d(\mathbf{k})_{\parallel} = M - 2B/a^2 + 2B(\cos k_x a + \cos k_y a - 2)/a^2$, Γ_i ($i = 0, 1, 2, 3$) are 4×4 Dirac matrices and $\mathbf{1}$ is the unit matrix of the same size. The numerical values of parameters are chosen as: $M = 0.3$ eV; $A = 0.5$ aeV; and $B = 0.25$ a^2 eV. The Fermi energy of the whole device is set at $E_F = 3.1$ eV, and the bottom of the band of the TI layer is shifted by $C = 3.0$ eV.

The hopping $\gamma_c = 0.25$ eV between F or N monolayers and the TI monolayer is chosen to ensure that the Dirac cone on the surface of TI is not distorted [13, 14] by the penetration of evanescent modes from these neighboring metallic layers. The weak F to TI coupling can be achieved by growing an ultrathin layer of a conventional band insulator, such as In_2Se_3 with large bandgap and good chemical and structural compatibility with Bi_2Se_3 where sharp heterointerfaces have already been demonstrated by molecular-beam epitaxy growth [31]. We assume that such layer is present and suppresses the magnetic proximity effect so that $\Delta_n = 0$ on the TI monolayer (denoted as F/TI interface in Fig. 1) that is closest to the F layer.

The early phenomenological modeling [23] of STT in noncollinear ferromagnetic multilayers was succeeded by more microscopic theories [21, 24–27, 32], often in combination with first-principles input about real materials [21, 24, 25, 32]. These theories have been focused on devices without SOC where STT is directly connected to the divergence of spin current as a consequence of the conservation of total spin. Thus, STT vector can be obtained simply from the local spin current at the N/F or I/F interface within F'/N/F spin valves or F'/I/F magnetic tunnel junctions (MTJs). Such local spin currents are typically computed using the Landauer-Büttiker scattering approach [25, 32] or the NEGF formalism [21, 24, 27]. However, these methodologies are

inapplicable to junctions with SOC within the free F layer, which has recently ignited search for efficient algorithms [19–21] that can compute STT in the presence of spin non-conserving interactions. The SOC can be introduced into the device by either bulk ferromagnets (as in F layers based on ferromagnetic semiconductors [7, 19, 20]) or due to the Rashba SOC at the I/F interface in devices with structural inversion asymmetry [7].

Using the operators $\hat{c}_{n\sigma}^\dagger$ ($\hat{c}_{n\sigma}$) which create (annihilate) electron with spin σ on monolayer n , we can introduce the two fundamental objects [33] of the NEGF formalism—the retarded $G_{nn'}^{r,\sigma\sigma'}(t,t') = -i\Theta(t-t')\langle\{\hat{c}_{n\sigma}(t), \hat{c}_{n'\sigma'}^\dagger(t')\}\rangle$ and the lesser $G_{nn'}^{<,\sigma\sigma'}(t,t') = i\langle\hat{c}_{n'\sigma'}^\dagger(t')\hat{c}_{n\sigma}(t)\rangle$ GF that describe the density of available quantum states and how electrons occupy those states, respectively. Here $\langle\ldots\rangle$ denotes the nonequilibrium statistical average [33]. In stationary problems, \hat{G}^r and $\hat{G}^<$ depend only on the time difference $t - t'$ or energy E after the Fourier transform.

In the absence of SOC, one can obtain STT in F'/N/F spin valves or F'/I/F MTJs by computing [27] the vector of spin current between two neighboring monolayers n and $n + 1$ coupled by the hopping parameter γ :

$$\mathbf{I}_{n,n+1}^S = \frac{\gamma}{4\pi} \int dE d\mathbf{k}_\parallel \text{Tr}_\sigma [\hat{G}_{n+1,n}^< - \hat{G}_{n,n+1}^<]. \quad (3)$$

The integration over \mathbf{k}_\parallel is required because of the assumed translational invariance in the transverse direction. Since for conserved spin current, the monolayer-resolved [25] STT is given by $\mathbf{T}_n = -\nabla \cdot \mathbf{I}^S = \mathbf{I}_{n-1,n}^S - \mathbf{I}_{n,n+1}^S$, the total torque on the free F layer is, $\mathbf{T} = \sum_{n=0}^\infty (\mathbf{I}_{n-1,n}^S - \mathbf{I}_{n,n+1}^S) = \mathbf{I}_{-1,0}^S - \mathbf{I}_{\infty,\infty}^S = \mathbf{I}_{-1,0}^S$ [27]. Here the subscripts -1 and 0 refer to the last monolayer of the N or I barrier and the first monolayer of the F layer, respectively. In the multilayers with SOC, such as those in Fig. 1, this methodology to get STT *becomes inapplicable* since spin current will not decay (i.e., $\mathbf{I}_{\infty,\infty}^S \neq 0$) if SOC is present in the bulk of the free F layer [20]. Also, spin current across the interface $\mathbf{I}_{-1,0}^S$ is *insufficient* to get STT if strong SOC is present directly at the interface.

To derive a general NEGF-based expression for the expectation value of the current-induced force, we start by assuming that the device Hamiltonian depends on a variable q which corresponds to slow collective classical degrees of freedom. The expectation value of the corresponding canonical force $\hat{Q} = -\partial\hat{H}/\partial q$ is obtained using the density matrix $\hat{\rho} = \frac{1}{2\pi i} \int dE \hat{G}^<(E, q)$:

$$Q = -\frac{1}{2\pi i} \int_{-\infty}^{+\infty} dE \text{Tr} \left[\frac{\partial\hat{H}}{\partial q} \hat{G}^< \right] = -\left\langle \frac{\partial\hat{H}}{\partial q} \hat{G}^< \right\rangle, \quad (4)$$

where $\hat{G}^<(E, q)$ is adiabatic GF obtained for a frozen-in-time variable q . By exchanging the derivative between the Hamiltonian and $\hat{G}^<(E, q)$, $Q = -\partial\langle\hat{H}\hat{G}^<\rangle/\partial q + \langle\hat{H}\partial\hat{G}^</\partial q\rangle$, and by using the standard equations for the

retarded and lesser GFs [33], $\hat{G}^r(E) = [E - \hat{H} - \hat{\Sigma}^r]^{-1}$ and $\hat{G}^<(E) = \hat{G}^r(E)\hat{\Sigma}^<(E)\hat{G}^a(E)$, we finally obtain

$$Q = i \left\langle \frac{\partial\hat{G}^r}{\partial q} \hat{\Sigma}^< \hat{G}^a \hat{\Gamma} \right\rangle - \left\langle \hat{\Sigma}^< \frac{\partial\hat{G}^r}{\partial q} \right\rangle. \quad (5)$$

where the advanced GF is given by $\hat{G}^a = [\hat{G}^r]^\dagger$. In the elastic transport regime, $\hat{\Gamma}(E) = \sum_p \hat{\Gamma}_p(E - eV_p)$ is the sum of the level broadening operators $\hat{\Gamma}_p(E - eV_p) = i[\hat{\Sigma}_p^r(E - eV_p) - \hat{\Sigma}_p^a(E - eV_p)]$; $\hat{\Sigma}_p^r(E - eV_p)$ are the self-energies due to the coupling to semi-infinite (F or N) ideal leads $p = L, R$; and $\hat{\Sigma}^<(E) = \sum_p i f_p(E) \hat{\Gamma}_p(E - eV_p)$ is the lesser self-energy [33]. The junction is biased by the voltage $V_b = V_L - V_R$ and $f_p(E) = f(E - eV_p)$ is the Fermi function of the macroscopic reservoir to which the lead p is assumed to be attached at infinity. We note that Eq. (5) is akin to the mean value of time-averaged force in nonequilibrium Born-Oppenheimer approaches [34] to current-induced forces exerted by conduction electrons on ions in nanojunctions or mechanical degrees of freedom in nanoelectromechanical systems whose collective modes are slow compared to electronic time scales.

The application of Eq. (5) to get T_α ($\alpha = x, y, z$) component of the STT vector acting on the magnetization of the free F layer within N/TI/F junction proceeds by first computing $\hat{G}^r(E)$ for the device described by the Hamiltonian $\hat{H} = \hat{H}_{\text{TI}} + \hat{H}_F$. In the second step, the Hamiltonian of the F layer is modified

$$\hat{H}_F^q = \hat{H}_F + q \sum_{n,\sigma\sigma',\mathbf{k}_\parallel} \hat{c}_{n\sigma,\mathbf{k}_\parallel}^\dagger [\mathbf{e}_\alpha \cdot (\mathbf{m} \times \hat{\sigma})]_{\sigma\sigma'} \hat{c}_{n\sigma',\mathbf{k}_\parallel}, \quad (6)$$

and $\hat{G}^r(E)[\hat{H}^q]$ is computed for the new Hamiltonian $\hat{H}^q = \hat{H}_{\text{TI}} + \hat{H}_F^q$. This yields $\partial\hat{G}^r/\partial q \approx (\hat{G}^r[\hat{H}^q] - \hat{G}^r[\hat{H}])/q$ where we use $q = 10^{-7}$ as the infinitesimal. The derivative $\partial\hat{G}^r/\partial q$ plugged into Eq. (5) yields $Q = T_\alpha$.

Equation (5) includes both the equilibrium $\mathbf{T}_\perp(V_b = 0)$ [21, 26, 27] and experimentally measured [3] *nonequilibrium* $\mathbf{T}_\perp(V_b) - \mathbf{T}_\perp(V_b = 0)$ contribution to \mathbf{T}_\perp . The linear-response contribution can be extracted (see Sec. III in [18]) by expanding the density matrix $\hat{\rho}$ to first order in the applied bias voltage V_b and by subtracting the purely equilibrium term $\hat{\rho}_{\text{eq}} = -\frac{1}{\pi} \int dE \text{Im} [\hat{G}_0^r(E)] f(E)$:

$$Q_{\text{neq}} = -\sum_p V_p \text{Tr} \left[\frac{\partial\hat{G}_0^r}{\partial q} \hat{\Gamma}_p \hat{G}_0^a \hat{\Gamma} - i \frac{\partial\hat{G}_0^r}{\partial q} \hat{\Gamma}_p \right] - \sum_p V_p \text{Im} \left\{ \int_{-\infty}^{E_F} dE \text{Tr} \left[\frac{\partial\hat{G}_0^r}{\partial q} \frac{\partial\hat{H}}{\partial V_p} - \frac{\partial\hat{G}_0^r}{\partial q} \frac{\partial\hat{\Sigma}_p^r}{\partial E} \right] \right\}. \quad (7)$$

Here $G_0^r(E)$ is the retarded GF at zero bias voltage and we assume zero temperature. The second sum in

Eq. (7) is non-zero only for $\mathbf{T}_\perp \propto V_b$ where the integration over the Fermi sea is necessary to ensure the *gauge invariance* (i.e., invariance under a global potential shift $V_p \rightarrow V_p + V_0$) of \mathbf{T}_\perp plotted in Fig. 2. Note that $\mathbf{T}_\perp \propto V_b$ component is identically zero [3, 26, 27] in symmetric F'/I/F MTJs, as confirmed by Fig. 2(b) using our general Eq. (7).

We conclude by noting that although STT we predict in N/TI/F junctions does not require F' layer with fixed magnetization as polarizer, its measurement necessitates usage of the second reference F' layer in order to detect magnetization switching or precession in the free F layer. Nevertheless, the experimental setups we propose for this purpose in Sec. II of [18], consisting of MTJ capped with TI layer to form TI/F/I/F' stacking, require much lesser total number of layers than recently fabricated orthogonal ST-MRAM [16] or ST oscillators [17] (containing F'' polarizer whose fixed magnetization must be kept perpendicular to in-plane magnetized F and F' layers).

F. M. and B. K. N. were supported by DOE Grant No. DE-FG02-07ER46374. N. N. was supported by Grant-in-Aids for Scientific Research (21244053) from the Ministry of Education, Culture, Sports, Science and Technology of Japan, Strategic International Cooperative Program (Joint Research Type) from Japan Science and Technology Agency, and also by Funding Program for World-Leading Innovative R&D on Science and Technology (FIRST Program).

* bnkolic@udel.edu

- [1] D. Ralph and M. Stiles, J. Magn. Magn. Mater. **320**, 1190 (2008); A. Brataas, A. D. Kent, and H. Ohno, Nature Mater. **11**, 372 (2012).
- [2] J. A. Katine and E. E. Fullerton, J. Magn. Magn. Mater. **320**, 1217 (2008).
- [3] C. Wang *et al.*, Nature Phys. **7**, 496 (2011).
- [4] I. M. Miron *et al.*, Nature Mater. **9**, 230 (2010); I. M. Miron *et al.*, Nature **476**, 189 (2011).
- [5] L. Liu *et al.*, Phys. Rev. Lett. **109**, 096602 (2012).
- [6] A. Manchon and S. Zhang, Phys. Rev. B **78**, 212405 (2008); A. Manchon and S. Zhang, *ibid.* **79**, 094422 (2009); K. Obata and G. Tatara, *ibid.* **77**, 214429 (2008); A. Matos-Abiague and R. L. Rodriguez-Suarez, *ibid.* **80**, 094424 (2009); I. Garate and A. H. MacDonald, *ibid.* **80**, 134403 (2009).
- [7] P. Gambardella and I. M. Miron, Philos. Transact. A Math. Phys. Eng. Sci. **369**, 3175 (2011).
- [8] M. Z. Hasan and C. L. Kane, Rev. Mod. Phys. **82**, 3045 (2010).
- [9] D. Pesin and A. H. MacDonald, Nature Mater. **11**, 409 (2012).
- [10] I. Garate and M. Franz, Phys. Rev. Lett. **104**, 146802 (2010); T. Yokoyama, J. Zang, and N. Nagaosa, Phys. Rev. B **81**, 241410(R) (2010); T. Yokoyama, Phys. Rev. B **84**, 113407 (2011).
- [11] F. Mahfouzi, J. Fabian, N. Nagaosa, and B. K. Nikolić, Phys. Rev. B **85**, 054406 (2012).
- [12] A. Manchon, Phys. Rev. B **83**, 172403 (2011).
- [13] F. Mahfouzi, N. Nagaosa, and B. K. Nikolić, arXiv:1112.2314.
- [14] E. Zhao, C. Zhang, and M. Lababidi, Phys. Rev. B **82**, 205331 (2010); J. A. Hutasoit and T. D. Stanescu, Phys. Rev. B **84**, 085103 (2011).
- [15] N. P. Butch *et al.*, Phys. Rev. B **81**, 241301 (2010); D. Kim *et al.*, Nature Phys. **8**, 460 (2012).
- [16] H. Liu *et al.*, Appl. Phys. Lett. **97**, 242510 (2010).
- [17] D. Houssameddine *et al.*, Nature Mater. **6**, 447 (2007).
- [18] See Supplemental Material at <http://link.aps.org/supplemental/>
- [19] K. M. D. Hals, A. Brataas, and Y. Tserkovnyak, EPL (Europhysics Letters) **90**, 47002 (2010).
- [20] P. M. Haney and M. D. Stiles, Phys. Rev. Lett. **105**, 126602 (2010).
- [21] P. M. Haney *et al.*, Phys. Rev. B **76**, 024404 (2007).
- [22] X. Jia, K. Xia, Y. Ke, and H. Guo, Phys. Rev. B **84**, 014401 (2011).
- [23] J. C. Slonczewski, J. Magn. Magn. Mater. **159**, L1 (1996); L. Berger, Phys. Rev. B **54**, 9353 (1996).
- [24] D. M. Edwards, F. Federici, J. Mathon, and A. Umerski, Phys. Rev. B **71**, 054407 (2005).
- [25] S. Wang, Y. Xu, and K. Xia, Phys. Rev. B **77**, 184430 (2008).
- [26] J. Xiao, G. E. W. Bauer, and A. Brataas, Phys. Rev. B **77**, 224419 (2008).
- [27] I. Theodonis *et al.*, Phys. Rev. Lett. **97**, 237205 (2006); Y.-H. Tang *et al.*, Phys. Rev. B **81**, 054437 (2010).
- [28] B. K. Nikolić and S. Souma, Phys. Rev. B **71**, 195328 (2005).
- [29] I. Adagideli, G. E. W. Bauer, and B. I. Halperin, Phys. Rev. Lett. **97**, 256601 (2006).
- [30] C.-X. Liu *et al.*, Phys. Rev. B **82**, 045122 (2010).
- [31] Z. Y. Wang *et al.*, Appl. Phys. Lett. **99**, 023112 (2011).
- [32] M. D. Stiles and A. Zangwill, Phys. Rev. B **66**, 014407 (2002).
- [33] H. Haug and A.-P. Jauho, *Quantum kinetics in transport and optics of semiconductors* (Springer, Berlin, 2007).
- [34] J.-T. Lü, M. Brandbyge, and P. Hedegård, Nano Lett. **10**, 1657 (2010); N. Bode, S. V. Kusminskiy, R. Egger, and F. von Oppen, Phys. Rev. Lett. **107**, 036804 (2011); N. Bode, L. Arrachea, G. S. Lozano, T. S. Nunner, and F. von Oppen, Phys. Rev. B **85**, 115440 (2012).